IEIE Transactions on Smart Processing and Computing, vol. 10, no. 2, April 2021
https://doi.org/10.5573/IEIESPC.2021.10.2.151

A Concurrent Triple-band RF Energy Harvesting Circuit for IoT Sensor Networks

Luong Duy Manh[1], Phan Thi Bich[1], Nguyen Thuy Linh[1], Nguyen Huy Hoang[1], Tran Xuan Nam[1], and Koichiro Ishibashi[2]

[1] Le Quy Don Technical University, 236 Hoang Quoc Viet, Hanoi, Vietnam
[2] The University of Electro-Communications, 1 Chome-5-1 Chofugaoka, Chofu, Tokyo 182-8585, Japan

* Corresponding Author: Luong Duy Manh, duymanhcs2@mta.edu.vn

Received August 30, 2020; Revised October 14, 2020; Accepted November 10, 2020; Published April 30, 2021

* *Regular Paper*

* *Extended from a Conference: Preliminary results of this paper were presented at the ICGHIT2020. This paper has been accepted by the editorial board through the regular reviewing process that confirms the original contribution.*

***Abstract*:** In this paper, a concurrent triple-band RF energy harvesting circuit is proposed. The proposed circuit incorporates a triple-band microstrip antenna combining a low-loss diplexer and three compact RF rectifiers. The proposed circuit operates concurrently at three popular frequency bands: GSM-900, GSM-1800, and 2.45 GHz. To improve output voltage and efficiency, three rectifiers are connected in a stacked topology. The simulated and measured results demonstrate that the circuit operates well in concurrent bands. Moreover, the proposed circuit exhibits a low-complexity structure and compactness in size. These advantages make the circuit a strong potential candidate for running low-power devices in IoT sensor networks.

***Keywords*:** RFEH, Antenna, Rectifier, Triple-band

1. Introduction

In the era of the 4th industrial revolution, the number of smart-radio devices is increasing remarkably, especially the number of wireless sensors used in wireless sensor networks; smart devices in IoT networks; body-mounted, wearable radio devices; and wireless sensors for monitoring drought, natural disasters, traffic sensors, etc. They are all low-power radio devices that are deployed with high density in the networks. One of the most critical requirements for these smart devices is the ability to remain in uninterrupted operation over long periods. This is because these radio devices are deployed in complex locations, such as inside the human body; in remote and inaccessible areas, such as riverbeds; in complex terrains, such as offshore seas and islands; or in the mountains, where access to electrical power sources or the replacement of DC power sources such as batteries is impossible or complicated. Besides, the DC battery has a certain lifespan, and replacement cannot be made immediately or when facing stringent challenges if the devices are deployed in hard-to-reach and remote locations or inside the human body. In terms of the environment, a battery is a chemical source that can be harmful. Hence, finding new sources of renewable energy, or alternative green energy sources, helps to protect the environment. These reasons have led to the emergence of research on renewable energy sources for running these sensor devices without the need for a battery. Recently, there has been research into energy harvesting techniques from various sources in the environment, including thermal energy [1, 2], solar energy [3, 4], and mechanical energy [5]. However, these energy sources depend largely on the weather, and they are not continuous. Although solar energy provides high power levels, it is only available when the sun is up. Wind power is difficult for body-mounted radio devices to access, and wind is not continuous or stable. Heat energy and oscillation power are small and not continuous. The biggest drawback to these renewable energy sources is the discontinuity. In addition to these sources, radio frequency (RF) energy has recently become a promising renewable energy source due to the increasing number of wireless signal sources in the environment, including mobile base stations [6], Wi-Fi [7], radio and television transmitters [8-10], Bluetooth, laptops, and mobile phones [11-14]. These RF energy sources are not only continuous but highly condensed in the environment. These superior advantages make this type of

energy source very promising for utilization in many realistic applications.

However, one of the major downsides of the RF energy source is relatively low power density, which is about 1 μW/cm^2. Hence, RF energy harvesting systems need to operate efficiently to supply sufficient power to smart devices or sensors in a network. Nevertheless, the existing RF energy harvesting systems now face inherent drawbacks such that efficient extraction of energy from RF sources cannot be fulfilled. The main drawbacks cover the following aspects: antennas with low impedance, low gain, low efficiency, and a narrow bandwidth; active devices with low-efficiency rectifying operations, resulting in low output voltages; impedance-matching circuits with a narrowband operation, which are less efficient in a multiband operation; or the total size of the system is bulky and not appropriate for practical applications. Various solutions have been introduced, and a lot of research has been reported for years on ways to surmount these drawbacks. In terms of multiband operation, in [15] the authors proposed a dual-band antenna for RF energy harvesting (RFEH) systems. The antenna operates concurrently in Wi-Fi bands: 2.45 GHz and 5 GHz. The antenna was fabricated on an RT/Duroid 5870 substrate. The radiation pattern is quasi-omnidirectional, but the size of this antenna is relatively large. Moreover, the output voltage is just on the order of 1 V, with very high input power from 0 dBm to 15 dBm. Such high input power is not suitable for harvesting ambient RF energy, because RF power from the environment is usually very low (basically below 0 dBm). In [16], the authors presented an RFEH system to operate in three bands (LTE 700 MHz, GSM 850 MHz, and ISM 900 MHz) using just a single circuit. The system was tested in Boston. This system employed an HSMS-285C zero-bias Schottky diode as the active device, and efficiency could reach as high as 45% with a low input power range from -25 dBm to -5 dBm. However, the system is very bulky, especially in the antenna, and thus, it is not appropriate for integrated applications and commercialization. Shen et al. [17] reported a triple-band rectifier operating in the GSM-900, GSM-1800, and UMTS-2100 bands. This circuit could achieve high efficiency of 40% at a power density greater than 500 μW/m^2. Although this circuit could offer relatively high efficiency in triple-band operation, its delivered output voltage is relatively small (0.6 V). Chandravanshi et al. proposed a triple-band differential rectenna for RF energy harvesting applications [18]. It operates in UMTL, the lower WLAN/Wi-Fi, and WiMAX bands. This circuit achieved a maximum efficiency of 53% at 2 GHz, 31% at 2.5 GHz, and 15.56% at 3.5 GHz. However, the circuit was not integrated, and the antenna gain was low. In terms of efficiency enhancement of a rectifier, the authors in [19] proposed a high-efficiency rectifier used with a fractal loop antenna. The rectifier could deliver an efficiency of 61%. The output DC voltage was 1.8 V with a 12 kΩ resistor for a 10 μW/cm^2 power density at 1.8 GHz. This was considered a compact and high-efficiency rectifier. Nevertheless, the output voltage was still low, and this rectifier worked only in a single band. Authors in [20] presented an RF energy harvester designed to maximize

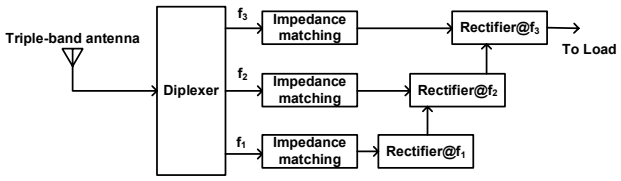

Fig. 1. Schematic of the proposed RFEH circuit.

harvested RF energy in the 902 MHz to 928 MHz bands. This harvester exhibited an efficiency of 32% at -15 dBm input power, with an output DC voltage of 3.2 V to a 1 MΩ load. This circuit offered relatively high efficiency and output voltage, but not in an integrated form, and moreover, it only operated in a narrow band.

In this paper, we develop a novel, compact, and low-cost RFEH circuit that operates concurrently in three frequency bands: GSM-900, GSM-1800, and 2.45 GHz. These are three of the most popular frequency bands with high-power density in the environment. If dual-band, the circuit might not have sufficient energy to power IoT sensors. Moreover, using quadruple-band or higher order circuits increases the complexity, thus increasing circuit size as well as losses in the PCB. The proposed circuit includes a compact triple-band antenna combining a low-loss diplexer and three rectifiers operating in each frequency band, as shown in Fig. 1. As indicated in the figure, the triple-band antenna, the low-loss diplexer, and the three rectifiers connect to each other in a stacked topology. This topology is employed to boost the output voltage efficiently, because the output voltage of the lower stage becomes the reference voltage of the next higher stage. The antenna was fabricated on a low-cost FR4 substrate for compact size and reduction of fabrication costs. In addition, the antenna was designed for simultaneous operation in the three frequency bands. The simulated and measured results demonstrate that the proposed RFEH circuit can obtain high efficiency at low input power, and provides high output voltage while still ensuring compactness in the entire circuit.

The rest of this paper is organized as follows: Section 2 presents the design procedure and simulated results for each part of the RFEH circuit, and then, experimental validation is presented in Section 3. Section 4 concludes the paper.

2. Circuit Design

In this section, the design of each part in the proposed circuit is presented. As shown in Fig. 1, the RFEH circuit consists of three main parts: the antenna, the diplexer, and the rectifiers. First, the design of the triple-band antenna is described.

2.1 Antenna Design

The antenna was designed and fabricated using microstrip technology on an FR4 substrate for its integration capability and low cost. The antenna operates concurrently in three bands: GSM-900, GSM-1800, and

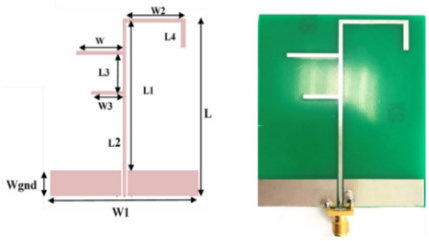

Fig. 2. Triple-band antenna layout in ADS (left) and in the fabricated prototype (right).

Table 1. Antenna dimensions.

Dimension	Value (mm)	Dimension	Value (mm)
L	90	Wgnd	10
L1	78.5	W	1.5
L2	30	W1	62.4
L3	14.3	S	0.5
L4	10	W2	26.5
W3	13.25	W4	19.5

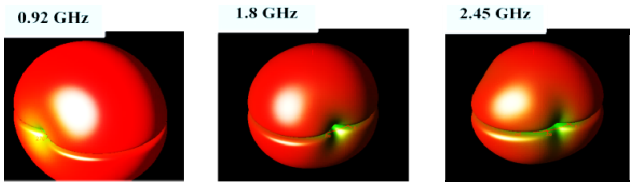

Fig. 3. Simulated radiation patterns of the triple-band antenna.

2.45 GHz. In addition to multi-band operation, the antenna is omnidirectional while still ensuring sufficient gain. The reason for being omnidirectional is that in realistic applications, the electromagnetic signal can come from any direction in the environment.

Fig. 2 shows the layout and fabricated prototype of the triple-band microstrip antenna. Here, the antenna is designed in the form of a microstrip dipole having reflective metal planes on the same layer as the dipole. The antenna includes three stubs with different lengths, which are used to tune the resonant frequency of the antenna to each operational frequency band. The first stub, with length W3, is tuned to the GSM-900 band, whereas the second, at length W, is tuned to the GSM-1800 band; the last, with a length of W2 + L, is tuned to the 2.45 GHz band. Note that the last stub is intentionally bent to save space. The width of the main microstrip line was chosen to be 0.5 mm, which is equivalent to a 50 Ω line. Dimensions of the antenna are given in Table 1.

To evaluate the antenna's performance for use in the RFEH circuit, we first checked the radiation pattern along with gain. This was done in an ADS2016 simulator using electromagnetic (EM) analysis.

In Fig. 3, which shows the radiation patterns of the designed antenna at each operation frequency, we see that the radiation pattern is omnidirectional at all operational frequencies. Simulated gain is 1.54 dBi at 920 MHz, 2.08 dBi at 1.8 GHz, and 3.02 dBi at 2.45 GHz. These

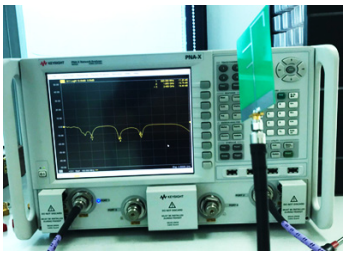

Fig. 4. Setup for return loss measurement.

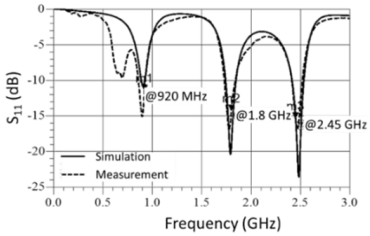

Fig. 5. Simulated and measured S_{11} results.

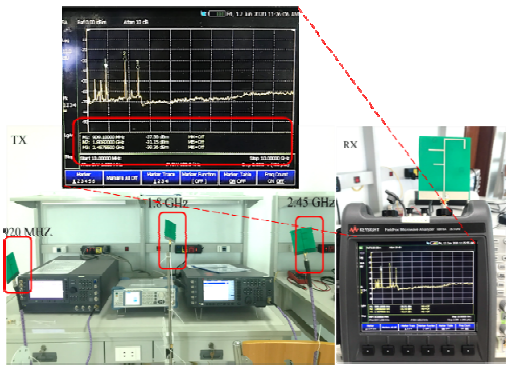

Fig. 6. A realistic experiment testing the antenna.

simulated results validate the appropriateness of the design. Here, the antenna was fabricated on the FR4 substrate with the following parameters: dielectric constant = 4.5, dissipation factor = 0.014, thickness = 0.8 mm, and copper thickness = 35 μm. Fig. 4 shows the experimental setup for evaluating the return loss of the fabricated antenna.

A vector signal analyzer (VNA) from Keysight (N5242A) was employed to measure the return loss (S_{11}) of the antenna to check the operational frequencies.

The simulated and measured results for S_{11}, shown in Fig. 5, imply that the antenna resonates at three frequencies: 920 MHz, 1.8 GHz, and 2.45 GHz, satisfying the requirement for multi-band operation. Moreover, we can also clearly see good agreement between the simulation and the measurements. This validates the accuracy of the design. There is some discrepancy between simulation and measurement at a lower frequency range (below 920 MHz) due to some errors from the calibration procedure. To further validate the antenna design, it was tested in a realistic experiment, shown in Fig. 6.

In the experiment, three signal generators connecting to the three antennas were employed to transmit three signals at the three operational frequencies: 920 MHz, 1.8 GHz, and 2.45 GHz. On the receiving side, the triple-band

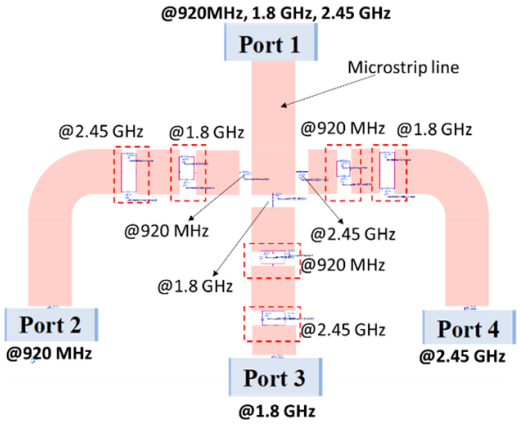

Fig. 7. Co-simulation model for the diplexer.

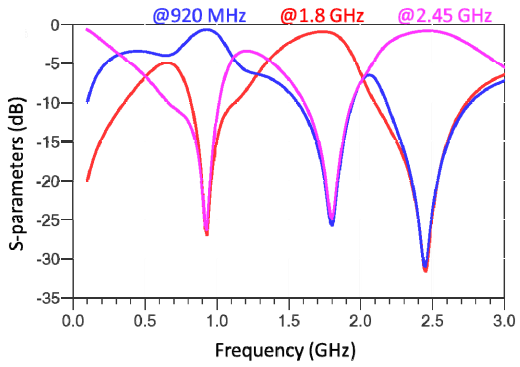

Fig. 8. Simulated S-parameters of the diplexer.

antenna was connected to a portable spectrum analyzer from Keysight. As seen in the figure, the antenna received all transmitted signals on the three operational frequency bands, as indicated by the received spectrum on the spectrum analyzer. This further validates the accuracy of the design.

2.2 Diplexer Design

The diplexer was designed to split the received signal into each signal at each operational frequency, which was then fed to each rectifier circuit. Therefore, it has to exhibit low loss and compactness. For compactness, the diplexer was designed using lumped components. Fig. 7 shows a co-simulation model for the diplexer, which was implemented in the ADS simulator. The model includes an EM model for microstrip lines functioning as interconnects, along with capacitors and inductors at three branches. Each branch consists of two parallel LC tanks combined with a lumped element, which is either an inductor or a capacitor.

Two LC tanks in each branch resonate at two resonant frequencies, and the other lumped element is tuned to pass the signal having the frequency of interest. Thanks to such a technique, the diplexer is able to pass the signal at each operational frequency to each branch. The total size of this circuit is just 1.8 cm × 2 cm. The simulated performance of the diplexer is in Fig. 8. We can see that the diplexer operates well at 920 MHz, 1.8 GHz, and 2.45 GHz. The insertion loss of each band is given as follows: -0.67 dB at

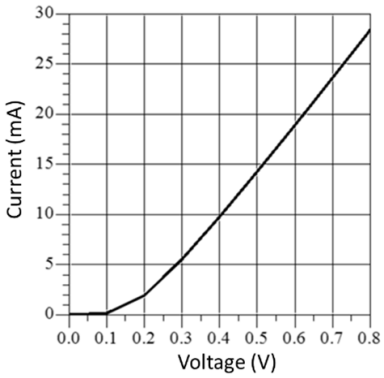

Fig. 9. I-V characteristics of the SMS7630 diode.

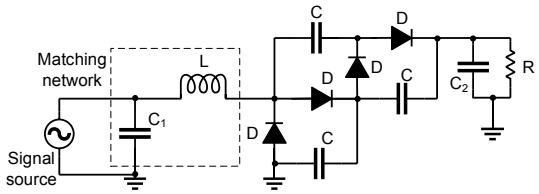

Fig. 10. Schematic of a single proposed rectifier.

920 MHz, -1.1 dB at 1.8 GHz, and -0.82 dB at 2.45 GHz. In addition, the figure also indicates that at each frequency band of interest, the signal on the other two bands is rejected, indicating a high isolation characteristic.

2.3 Rectifier Design

The rectifier is one of the most critical parts of the proposed RFEH circuit. In this study, the rectifier incorporates a matching network and a two-stage voltage-doubler circuit, where each stage uses two zero-bias SBD diodes (SMS7630). Here, the matching network was designed for each operational frequency band and at the same input power of -10 dBm to guarantee that the circuit can be used to collect RF energy from the environment. The SMS7630 was chosen because of its low cost and relatively low threshold voltage, as indicated in Fig. 9, which shows the I-V curve of this diode.

We can see in the figure that the threshold voltage of the SMS7630 is about 0.1 V. This implies the diode is highly suitable for RFEH applications. The schematic of the single rectifier operating in a single band, which was implemented in the ADS simulator, is shown in Fig. 10. The rectifier was implemented on the same FR4 substrate as the antenna and the diplexer, so all the parts of the RFEH circuit can be integrated on the same substrate. As mentioned previously, the output voltage of the 920 MHz rectifier becomes the reference voltage for the 1.8 GHz rectifier, and then, the output voltage of the 1.8 GHz rectifier becomes the reference voltage for the 2.45 GHz rectifier. A rectifier at 920 MHz was chosen as the first stage since the power level of this band is normally highest among the three bands, and this prevents the circuit from floating at the first stage. The entire RFEH circuit, which is realized by incorporating all the constituent parts, is illustrated in Fig. 11. Here, the matching network in the

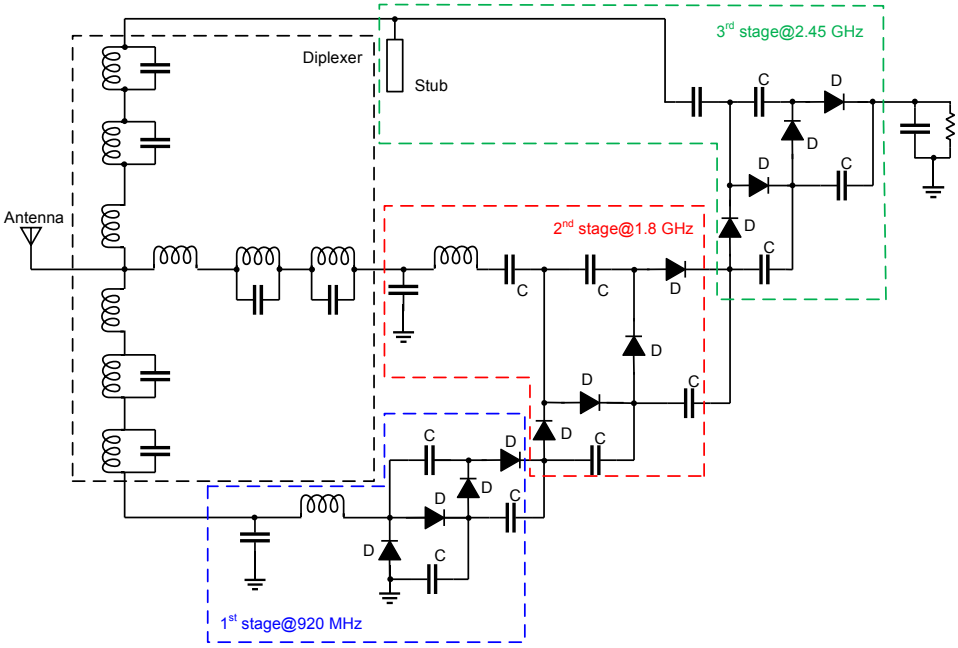

Fig. 11. Schematic of the entire RFEH circuit.

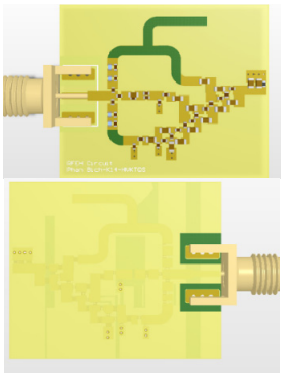

Fig. 12. Layout of the final RFEH circuit: top layer (upper) and bottom layer (lower).

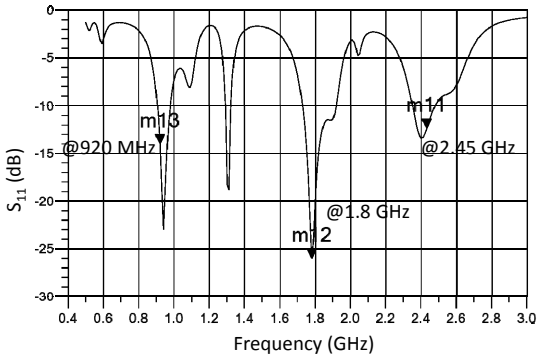

Fig. 13. Simulated return loss of the rectifier.

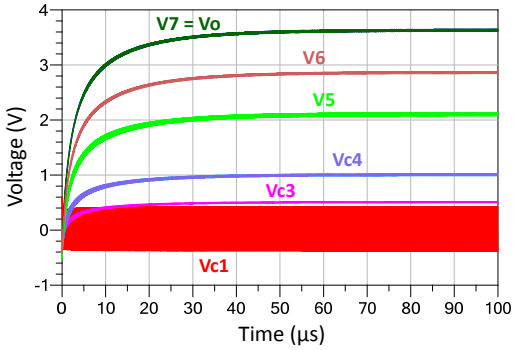

Fig. 14. Simulated voltage at each node of the circuit.

2.45 GHz rectifier branch uses an open stub for impedance matching, instead of lumped elements.

The layout of the final circuit for the schematic shown in Fig. 11, which was implemented in the Altium simulator, is shown in Fig. 12. The total size of the RFEH circuit is just 2 cm × 2 cm. Fig. 13 shows the simulated return loss of the rectifier in the ADS simulator to validate impedance matching at each operational frequency band. The simulated results indicate that the rectifier exhibits a reasonable return loss below -10 dB at each frequency band of interest. This clearly validates the design.

Thanks to the use of the stacked structure for the voltage doubler at each frequency band in each rectifier, output DC voltage can be significantly improved, as indicated in Fig. 14.

Fig. 14 presents the simulated voltage at each node, as shown in Fig. 11. We can see that Vc1 is an AC voltage, while the voltages at other nodes (Vc3, Vc4, V5, V6, and V7) are rectified voltages, and are thus DC. The DC voltage of the upper stage has a higher value, compared to the lower stage, as explained previously. The final output DC voltage (V7 or Vo) can be relative (more than 3.5 V) at an input level of -10 dBm. Additionally, the RF-DC efficiency of the proposed RFEH circuit is shown in Fig. 15.

We can see that the rectifier can achieve high efficiency due to the high output voltage. More than 60%

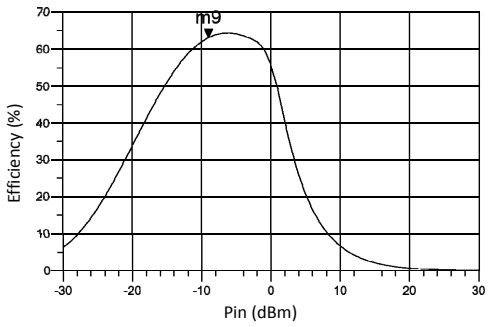

Fig. 15. Simulated RF-DC efficiency of the rectifier.

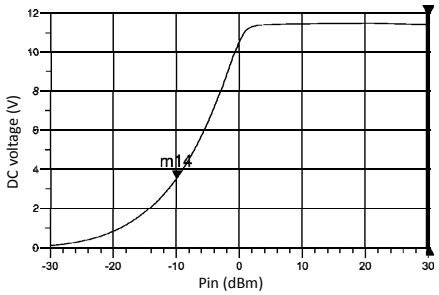

Fig. 16. Simulated output voltage with input power.

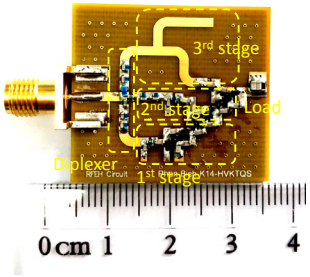

Fig. 17. Fabricated prototype of the RFEH circuit.

efficiency at -10 dBm input is clearly seen in the figure. Here, the value of the load resistor is 200 kΩ.

The output voltage can be increased much more if the collected input power is higher than -10 dBm, as demonstrated in Fig. 16. We can clearly see that the DC voltage is obtainable from 3.8 V to 10.5 V, when input power varies from -10 dBm to 0 dBm.

3. Experiment

The fabricated RFEH PCB is shown in Fig. 17. The circuit was fabricated on a low-cost and moderate-performance FR4 substrate. The total size is very compact: 2 cm × 2 cm.

To test the performance of the circuit, its return loss was first checked without connecting the antenna.

Fig. 18 shows the measured return loss of the rectifier circuit without the antenna connected. The designed circuit exhibits a relatively low return loss on the three bands of interest (GSM-900, GSM-1800, and 2.45 GHz). Note that the measured S_{11} slightly shifts over the simulated one due

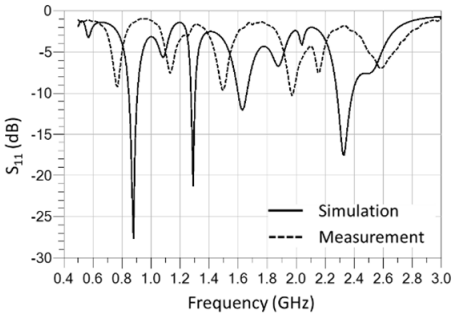

Fig. 18. Measured return loss of the RFEH circuit.

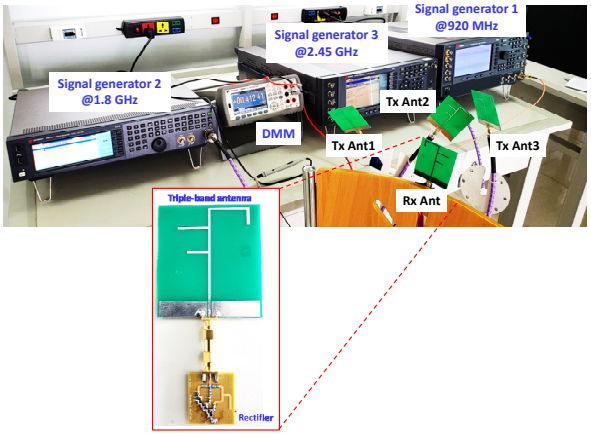

Fig. 19. Experimental setup for output DC voltage measurement.

to tolerance in the fabrication process of the microstrip PCB.

Fig. 19 shows the experimental setup for the measurement of output DC voltage from the designed RFEH circuit connecting the triple-band antenna. Here, three Keysight RF signal generators (SGs) are connected to three triple-band transmitting antennas (Tx Ant1, Tx Ant2, and Tx Ant3) to generate an RF signal on the three bands. The receiving circuit is the proposed rectifier connecting the triple-band receiving antenna (Rx Ant) through a male SMA–male SMA adapter. The output DC voltage was measured using a digital multimeter (DMM) from Keysight. All four antennas pointed towards each other to increase the received signal strength. RF power of each SG was 10 dBm, and the measured power at the receiving antenna was -22 dBm. The distance between Tx and Rx was 20 cm. The received RF power was measured directly from the Rx antenna connected to a spectrum analyzer. This low received power was caused by various loss factors, including antenna polarization mismatch, connector loss, and return loss of the antenna. The efficiency was calculated to be 12% at a received power of -22 dBm on a 200 kΩ load.

The measured results are indicated in Fig. 20 for various states of the SGs. We can see that when alternately turning on each SG at the corresponding frequency band, the output DC voltage is very low (that is, 0.2 V at 920 MHz, 0.04 V at 1.8 GHz, and 0.08 V at 2.45 GHz). However, when turning on all SGs simultaneously, the

Fig. 20. Measured output DC voltage according to different states of RF signal generators.

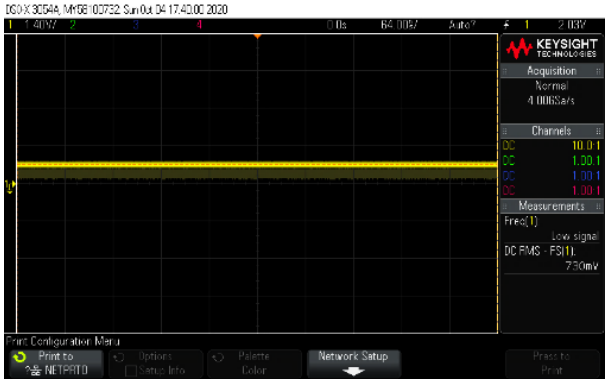

Fig. 21. Measured output voltage waveform.

Fig. 22. Detailed information of the measured output voltage waveform shown in Fig. 21.

output DC voltage increases significantly (to about 0.64 V), which implies that the designed circuit operates well on the three frequency bands concurrently. Nevertheless, the output DC voltage is still small compared with the simulation. This was probably caused by inaccuracies in the diode model in the ADS and from the PCB fabrication process.

Figs. 21 and 22 show the measured output voltage waveform of the circuit prototype.

Fig. 21 shows the voltage waveform on a Keysight DSOX3054A digital oscilloscope, and Fig. 22 indicates the detailed information of this waveform. Observe that the waveform is low-frequency, indicating the rectifying behavior, and the DC RMS value is 700 mV, which is the measured output rectified voltage.

Table 2. Performance comparison.

Related work	*RF source*	*RF power sensitivity*	*Output voltage*	*Size*	*Range/ antenna gain*	*Technology*
This work	GSM900; GSM180; WiFi	-22 dBm	0.64 V	8 cm x 11 cm (W x L)	20 cm/(1.5 dBi; 2 dBi; 3 dBi)	SMS-7630
Bakkali, *et al.* [21]	WiFi (2.45 GHz, 5 GHz)	10 dBm	1.3 V	NA	60 cm/4 dBi	SMS-7630-079LF
Dey, *et al.* [22]	GSM900; GSM180 0	NA	0.04 V – 0.09 V	NA	NA	HSMS-2850
Kim, *et al.* [23]	881 MHz; 2.4 GHz	22 dBm	6.8 V – 7.0 V	3 cm x 2.5 cm (w/o antenna)	From SG	HSMS-2822
Rengalakshmi, *et al.* [24]	GSM900	-10 dBm	0.6 V	NA	From SG (simulation)	HSMS285X

Table 2 compares the performance of the present study with other recent works.

We can see that the proposed circuit delivers a moderate voltage when collecting RF energy from the ambient environment, with a relatively low RF power of -22 dBm, while still ensuring the compact size of the entire circuit. However, the distance between the Tx and Rx was still short, due to the low gain in the designed antenna.

4. Conclusion

In this paper, a novel concurrent triple-band RFEH circuit is proposed for potentially running low-power sensors in IoT sensor networks. The proposed circuit operates concurrently on three popular frequency bands: GSM-900, GSM-1800, and 2.45 GHz. All parts in the circuit are implemented on the same low-cost FR4 substrate. The output DC voltage and the efficiency of the circuit are improved by using a stacked structure for the three rectifiers. Simulation and measurement validated the proposed design methodology and the performance of the RFEH circuit. The measured output for DC voltage of the circuit is about 643 mV when collecting RF signals simultaneously from the three SGs at 920 MHz, 1.8 GHz, and 2.45 GHz. The final sizes of the triple-band antenna and the rectifier circuit are 9 cm × 6.2 cm and 2 cm × 2 cm, respectively. Therefore, the proposed circuit is a promising candidate for running low-power sensors in IoT sensor networks.

Acknowledgement

This publication is the output of the ASEAN IVO (http://www.nict.go.jp/en/asean_ivo/index.html) project, “An Energy Efficient, Self-Sustainable, and Long Range IoT System for Drought Monitoring and Early Warning”, and financially supported by NICT (http://www.nict.go.jp/en/index.html).

References

[1] L. Mateu, et al., “Energy harvesting for wireless communication systems using thermo-generators,” in *Proc. of the 21st Conference on Design of Circuits and Integrated Systems (DCIS ’06)*, Barcelona, Spain, Nov. 2006.

[2] H. Bottner, et al., “New thermoelectric components using microsystem technologies,” *Journal of Micro-electromechanical Systems*, Vol. 13, No. 3, pp. 414–420, Jun. 2004. Article (CrossRef Link)

[3] C. Wang, et al., “Combining Solar Energy Harvesting with Wireless Charging for Hybrid Wireless Sensor Networks”, *IEEE Transactions on Mobile Computing*, Vol. 17, No. 3, Mar. 2018. Article (CrossRef Link)

[4] B. Mulla, et al., “Multiband Metamaterial Absorber Design Based on Plasmonic Resonances for Solar Energy Harvesting”, *Plasmonics*, No. 11, pp. 1313–1321, 2016. Article (CrossRef Link)

[5] S. Kim, et al., “Electrochemically driven mechanical energy harvesting”, *Nat Commun*, No. 7, 2016. Article (CrossRef Link)

[6] S. Kitazawa, et al., “Energy harvesting from ambient RF sources,” in *IEEE MTT-S Int. Microw. Symp. Workshop*, pp. 39–42, Jun. 2012. Article (CrossRef Link)

[7] Y. Shi, et al., "Design of a Novel Compact and Efficient Rectenna for WiFi Energy Harvesting," *Progress In Electromagnetics Research C*, Vol. 83, pp. 57-70, 2018. Article (CrossRef Link)

[8] T. Sogorb, et al., “Studying the feasibility of energy harvesting from broadcast RF station for WSN,” in *Proc. of the IEEE Instrumentation and Measurement Technology Conference Proceedings (IMTC ’08)*, pp. 1360–1363, IEEE, Victoria, Canada, May 2008. Article (CrossRef Link)

[9] T. S. Salter, “Low power smart-dust receiver with novel applications and improvements of an RF power harvesting circuit”, *[Ph.D. thesis]*, University of Maryland, 2009.

[10] C. Mikeka, et al., “Sustainable energy harvesting technologies—past, present and future,” in *Design Issues in Radio Frequency Energy Harvesting System*, Ed., InTech, Vienna, Austria, 2011.

[11] T. B. Lim, et al., “Feasibility study on ambient RF energy harvesting for wireless sensor network,” in *Proc. of the IEEE MTT-S International Microwave Workshop Series on RF and Wireless Technologies for Biomedical and Healthcare Applications (IMWS-BIO ’13)*, pp. 1–3, IEEE, Singapore, Dec. 2013. Article (CrossRef Link)

[12] S. N. Deepa, et al., “RF energy harvesting using 900MHz of mobile signal frequency to charging the mobile battery”, in *Proc. of 2017 International Conference on Innovations in Green Energy and Healthcare Technologies (IGEHT)*, Coimbatore, India, pp. 16-18, Mar. 2017. Article (CrossRef Link)

[13] M. Arrawatia, et al., "Broadband rectenna array for RF energy harvesting," in *Proc. of 2016 IEEE International Symposium on Antennas and Propagation (APSURSI)*, pp. 1869-1870, Oct. 2016. Article (CrossRef Link)

[14] M. J. M. Silva, et al., "Radio frequency energy harvesting using series resonant circuit," in *Proc. of 2017 IEEE 18th Wireless and Microwave Technology Conference (WAMICON)*, Cocoa Beach, FL, pp. 1-4, May 2017. Article (CrossRef Link)

[15] A. Bakkali, et al., “A Dual-Band Antenna for RF Energy Harvesting Systems in Wireless Sensor Networks”, *Journal of Sensors*, Vol. 2016, 2016. Article (CrossRef Link)

[16] U. Muncuk, et al., "Multiband Ambient RF Energy Harvesting Circuit Design for Enabling Battery-less Sensors and IoT," *IEEE Internet of Things Journal*, Vol. 5, No. 4, pp. 2700-2714, Aug. 2018. Article (CrossRef Link)

[17] S. Shen, et al., "A Dual-Port Triple-Band L-Probe Microstrip Patch Rectenna for Ambient RF Energy Harvesting," *IEEE Antennas and Wireless Propagation Letters*, Vol. 16, pp. 3071-3074, Oct. 2017. Article (CrossRef Link)

[18] S. Chandravanshi, et al., "Design of Dual Band Compact Wireless Energy Harvesting Circuit for GSM and WLAN Band," in *Proc. of 2018 IEEE MTT-S International Microwave and RF Conference (IMaRC)*, Kolkata, India, pp. 1-4, Nov. 2018. Article (CrossRef Link)

[19] M. Zeng, et al., "A Compact Fractal Loop Rectenna for RF Energy Harvesting," *IEEE Antennas and Wireless Propagation Letters*, Vol. 16, pp. 2424-2427, Jul. 2017. Article (CrossRef Link)

[20] Z. Hameed, et al., “Design of impedance matching circuits for RF energy harvesting systems”, *Micro-electronics Journal*, Vol. 62, pp. 49-56, Apr. 2017. Article (CrossRef Link)

[21] A. Bakkali, et al. "A Dual-Band Antenna for RF Energy Harvesting Systems in Wireless Sensor Networks," *Journal of Sensors*, Vol. 2016, Article ID 5725836, 8 pages, 2016. Article (CrossRef Link)

[22] K. Dey, et al. " Design of dual band rectifiers for energy harvesting applications," in *Proc. of 2018 International Applied Computational Electromagnetics Society Symposium (ACES)*, Denver, CO, USA, Mar. 2018. Article (CrossRef Link)

[23] P. Kim, et al. "A dual-band RF energy harvesting using frequency limited dual-band impedance matching," *Progress In Electromagnetics Research*, Vol. 141, pp. 443-461, 2013. Article (CrossRef Link)

[24] P. Rengalakshmi, et al. "Rectifier for RF Energy Harvesting," *International Journal of Computer Applications*, Vol. 143, No. 10, 2016. Article (CrossRef Link)

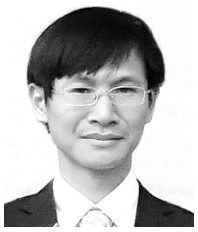

Luong Duy Manh received a BSc and an MSc in Physics in 2005 and 2007, respectively, from Hanoi University of Science (HUS), which is affiliated with Vietnam National University (VNU), Hanoi, Vietnam, and received a D.Eng. in Electronics Engineering from the University of Electro-Communications (UEC), Tokyo, Japan, in March 2016. He worked at the Graduate School of Engineering Science, Osaka University, Japan, as a postdoctoral researcher from April 2016 to June 2017. He is currently a lecturer at Le Quy Don Technical University, Hanoi, Vietnam. His research interests include development of microwave semiconductor devices and circuits, and terahertz (THz) integrated systems for wireless communications applications based on resonant tunneling diodes (RTDs) and photonic crystals.

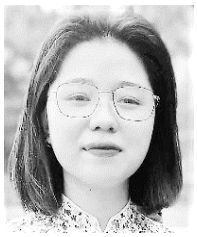

Phan Thi Bich received an M.Eng. from Le Quy Don Technical University, Hanoi, Vietnam, in 2020 in Electronics Engineering. She is now working at Ace Antenna Co., Ltd. Her research interests include design of waveguide filters and semiconductor circuits.

Nguyen Thuy Linh received a B.Eng. and an M.Eng. in Electronics Engineering from Le Quy Don Technical University, Hanoi, Vietnam, in 2009 and 2013, respectively, and received a D.Eng. in Electronics Engineering from the University of Electro-Communications (UEC), Tokyo, Japan, in March 2020. She is currently a lecturer at Le Quy Don Technical University, Hanoi, Vietnam. Her research interests include development of RF energy harvesting systems using CMOS technology.

Nguyen Huy Hoang received a B.Eng., an M.Eng., and a D.Eng. in Electronics Engineering from Le Quy Don Technical University, Hanoi, Vietnam, in 1996, 1999, and 2006, respectively. He is currently head of the Radio Engineering Fundamental Department at Le Quy Don Technical University, Hanoi, Vietnam. His research interests include design of RF and microwave circuits.

Xuan Nam Tran (Member, IEEE) received a Master of Engineering degree in telecommunications engineering from the University of Technology Sydney, Ultimo, NSW, Australia, in 1998, and a Doctor of Engineering degree in electronic engineering from The University of Electro-Communications, Chofu, Japan, in 2003. He is currently a Full Professor and the Head of a strong research group on advanced wireless communications with Le Quy Don Technical University, Hanoi, Vietnam. From November 2003 to March 2006, he was a Research Associate with the Information and Communication Systems Group, Department of Information and Communication Engineering, at the University of Electro-Communications. Since 2006, he has been with Le Quy Don Technical University. His research interests are in the areas of space-time signal processing for communications in fields such as adaptive antennas, space-time coding, MIMO, spatial modulation, and cooperative communications. He was the recipient of the 2003 IEEE AP-S Japan Chapter Young Engineer Award, and was a co-recipient of two best paper awards from the 2012 International Conference on Advanced Technologies for Communications and the 2014 National Conference on Electronics, Communications and Information Technology. He is the founding Chair and is currently the Chapter Chair of the Vietnam Chapter of the IEEE Communications Society. He is a member of IEICE and the Radio-Electronics Association of Vietnam (REV).

Koichiro Ishibashi received a PhD from the Tokyo Institute of Technology, Tokyo, Japan, in 1985 in Applied Electronics. After that, he joined the Central Research Laboratory, Hitachi Ltd., in 1985, where he investigated low-power technologies for SH microprocessors and high-density SRAMs. He worked for Renesas Electronics from 2004 to 2011, where he developed low-power IPs, mainly for SOCs used in mobile phones. He has been a Professor at The University of Electro-Communications, Tokyo, Japan, since 2011. He has presented more than 150 papers at international conferences, and has published papers in numerous journals. He was awarded the R&D 100 for the development of the SH4 Series Microprocessor in 1999. He is a Member of IEICE and a Fellow of IEEE. His current research interests include IoT technologies, including ultra-low power LSI design technology, technologies for energy-harvesting sensor networks and applications, and bio sensor technology.